Наносистеми, наноматеріали, нанотехнології
Nanosistemi, Nanomateriali, Nanotehnologii
2026, т. 24, № 2, сс. 597–606
https://doi.org/10.15407/nnn.24.02.0597

PACS numbers: 61.43.Gt, 62.20.Qp, 62.23.Pq, 81.05.Rm, 81.07.Wx, 81.20.Ev, 81.70.Bt

Study of the Effect of Adding Nanocarbon on the Mechanical Properties of Aluminium Pistons Using the Powder-Metallurgy Method

Shahad Mozar Sameen and Ibrahim Khalaf Salman

College of Education for Pure Sciences,
Department of Physics,
Tikrit University,
Tikrit, Iraq

In this work, aluminium is combined with carbon nanomaterials to enhance the mechanical properties of aluminium–carbon alloys, using powder-metallurgy technology. The powders are mixed in specific weight ratios and varying reinforcement concentrations, with aluminium serving as the base material and carbon nanomaterials as the reinforcement. These powders are pressed into moulds with a diameter of 10 mm, producing six samples of aluminium–carbon-alloy compacts. The mechanical properties of the prepared samples, such as hardness, porosity, and density, are studied. The best hardness value achieved is of 32.5 g/mm^2. As observed, porosity increases with the reinforcement content after the second sample, while reinforcement content inversely affects both bulk and apparent densities, decreasing them as the reinforcement content is increased.

У даній роботі алюміній було поєднано з вуглецевими наноматеріялами для поліпшення механічних властивостей алюмінійово-вуглецевих стопів за допомогою технології порошкової металурґії. Порошки змішували у певних вагових співвідношеннях і з різною концентрацією армування, причому алюміній служив основним матеріялом, а вуглецеві наноматеріяли — арматурою. Ці порошки пресували у форми діаметром у 10 мм, одержуючи шість зразків компактних заготівок зі стопу алюміній–вуглець. Було досліджено механічні властивості підготовлених зразків, такі як твердість, пористість і густина. Найліпше досягнуте значення твердости становило 32,5 г/мм^2. Було відзначено, що пористість збільшувалася зі збільшенням вмісту арматури після другого зразка, тоді як вміст арматури впливав обернено як на об'ємну, так і на видиму густину, зменшуючи їх зі збільшенням вмісту арматури.

Key words: aluminium, nanocarbon, density, porosity, hardness, powder metallurgy, sintering.

Ключові слова: алюміній, нановуглець, густина, пористість, твердість, порошкова металурґія, спікання.

(Received 17 December, 2024; in revised form, 22 December, 2024)

1. INTRODUCTION

Composite materials are composed of two or more materials combined together. One of these materials is called the matrix, which typically has a lower density, such as aluminium or titanium. The other is the reinforcement, which may consist of particles, filaments, or fibres. Composite materials exhibit superior mechanical properties and higher performance compared to individual materials used alone [1]. This makes them suitable for a wide range of engineering applications, including automotive, machinery, military tools, shipbuilding, aerospace, and more [2, 3]. These materials are characterized by their lightweight, high strength [4, 5], thermal stability, thermal conductivity, hardness, and low thermal-expansion coefficient [6, 7].

Various metals, such as copper, magnesium, aluminium, and titanium, are commonly used as matrix materials in metal-matrix composites (MMCs) [8]. Among these, aluminium-based MMCs are the most widely used [9] due to their high hardness, excellent damping capabilities, outstanding thermal management properties, lightweight nature, and good corrosion resistance [10]. Aluminium-based MMCs find applications in diverse fields such as lightweight designs (*e.g.*, in automotive, aerospace, railways, marine industries, and aircraft), high-temperature components (*e.g.*, pistons, cylinders, bearings, and connecting rods), electronic and thermal management packaging, and electrical and thermal transport systems [11].

Both micro- and nanoscale reinforcement materials are utilized in various applications. Common examples of microscale reinforcements include AlN, Al_2O_3, SiC, ZrO_2, Si_3N_4, TiB_2, and Y_2O_3. Similarly, nanoscale reinforcements include carbon nanomaterials, SiC nanoparticles, ZrO_2 nanoparticles, and fullerenes [12]. Microscale reinforcements in aluminium-based materials improve the mechanical properties of composites. However, further enhancement in strength can be achieved by reducing the reinforcement size to the nanoscale. Nanoscale reinforcements interact more effectively at the interface with the matrix material. When aluminium is reinforced with nanomaterials, it results in significant improvements in properties such as ultimate tensile strength, yield strength, and Young's modulus [13].

Aluminium-matrix composites (AMCs) are produced, using various manufacturing processes such as powder metallurgy, spark

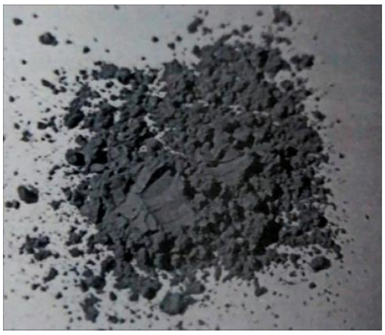

Fig. 1. Aluminium powder.

Fig. 2. Nanocarbon powder.

plasma sintering (SPS), stir casting, friction stir processing, and severe plastic deformation [14].

Powder metallurgy is a simple and cost-effective method that has proven effective in uniformly dispersing reinforcements within the aluminium matrix, as well as enhancing the mechanical properties of the composite [15].

2. PRACTICAL ASPECTS

2.1. Raw Materials

Aluminium powder: a 100-g aluminium powder with a purity of (99.1%), sourced from Thomas Baker (India), as shown in Fig. 1. Carbon nanomaterial: a 50-g carbon nanomaterial with a purity of (99.5%), obtained from (Avonchem UK), as shown in Fig. 2.

2.2. Procedure: Preparation of the Mixture

The mixture proportions were calculated based on the volumetric ratio of each component, considering the density difference between aluminium and carbon nanomaterials. A Sartorius analytical balance (Japan-made) with an accuracy of 0.0001 g was used for weighing, as shown in Fig. 3.

A 2-g sample was prepared for each compact as shown in Fig. 4 and distributed as detailed in Table 1.

2.3. Mixing Process

The measured quantities were placed in an agate mortar as shown in Fig. 5 and thoroughly mixed to achieve a homogeneous blend.

Fig. 3. A sensitive balance for measuring masses of samples.

Fig. 4. Compressed after pressing.

TABLE 1. The compresses and the percentage of each element in them.

Samples	m, g	
	Al	C
1	2	0.0
2	1.9	0.1
3	1.8	0.2
4	1.7	0.3
5	1.6	0.4
6	1.5	0.5

3. COMPACTION

The samples were formed by pressing the mixture, using uniaxial pressing at a force of 8 tons for 5 min. A hardened steel die as shown in Fig. 6 was used for this purpose.

4. TESTING METHODS

4.1. Hardness Testing

The Vickers microhardness test was conducted in a French METKON hardness device located at Tikrit University, College of Engineering, and shown in Fig. 7, which consists of an implantation tool, which is a pointed microscopic head in the shape of a square-base diamond pyramid, the levels of which intersect at the top at an angle of 136°, where the piston is fixed under this tool. A load of 500 g is applied for a time of 5 sec. The Vickers hardness number is calculated by measuring the lengths of the two diameters, d_1, d_2, and their average value, d_{av}, and applying the following relationship

Fig. 5. An agate mortar for grinding.

Fig. 6. Solid steel mould.

Fig. 7. Vickers hardness meter.

[16]:

$$HV = \frac{2P\sin(136°/2)}{d_{av}} = 1.854\frac{P}{d_{av}}, \quad (1)$$

where HV is Vickers hardness, P is applied pressure [N], d_{av} is average diameter of the mark. The hardness was taken at different areas such as the edges and the centre to obtain an approximate value for the hardness rate in units of [g/mm^2].

4.2. Apparent and Bulk Densities

The compacts were immersed in distilled water at room temperature for 24 hours. After immersion, they were removed, and any remaining surface water was wiped off. The saturated weight (W_s) was recorded. The samples were then suspended and submerged in distilled water, using a sensitive suspension balance located in the College of Education, University of Tikrit, to measure the suspended weight (W_i). Using the dry weight (W_d) and suspended weight (W_i), the apparent density (ρ_a) and bulk density (ρ_b) were calculated, using the following formulas [17, 18]:

$$\rho_a = \frac{W_d}{W_d - W_i}\rho_w , \quad (2)$$

$$r_b = \frac{W_d}{W_s - W_i}\rho_w , \quad (3)$$

where ρ_a is apparent density [g/cm^3], ρ_w is water density of 1000 g/cm^3, W_d is dry weight of the sample [*g*], W_i is suspended weight of the sample [*g*], ρ_b is bulk density [g/cm^3], W_s is saturated weight of the sample [*g*].

4.3. Apparent and True Porosity

Porosity was evaluated using the Archimedes principle. The dry weight (W_d) was recorded, followed by immersion in distilled water for 24 hours to measure the saturated weight (W_s). The samples were then suspended in distilled water to measure the suspended weight (W_i). Apparent porosity (*A.P.*) and true porosity (*T.P.*) were calculated as follows [19]:

$$A.P. = \frac{W_s - W_d}{W_s - W_i}\cdot 100\% , \quad (4)$$

$$T.P. = \frac{\rho_a - \rho_b}{\rho_a}\cdot 100\% . \quad (5)$$

5. RESULTS AND DISCUSSION

5.1. Vickers Hardness

The hardness values for the compacted samples with varying carbon nanomaterial content are shown in Table 2 and Fig. 8 The highest Vickers hardness value of 32.5 g/mm^2 was achieved by sample 2 with a carbon content of 0.1 g. Hardness decreases as the carbon content increases beyond 0.1 g, with the lowest value of 20.1 g/mm^2 observed for sample 6 (with 0.5 g carbon content). This decrease in hardness is attributed to the reduced base-material content, the formation of new phases during mixing and compaction, and increased interfacial surface area due to added reinforcement.

5.2. Apparent and True Porosity

Table 3 shows the nanocarbon content and the apparent and true porosity values for the compressed samples. The lowest porosity

TABLE 2. Hardness values and carbon content in the samples.

No. of samples	Content of C, g	Hardness, g/mm^2
1	0	25.2
2	0.1	32.5
3	0.2	26.9
4	0.3	23.9
5	0.4	21.8
6	0.5	20.1

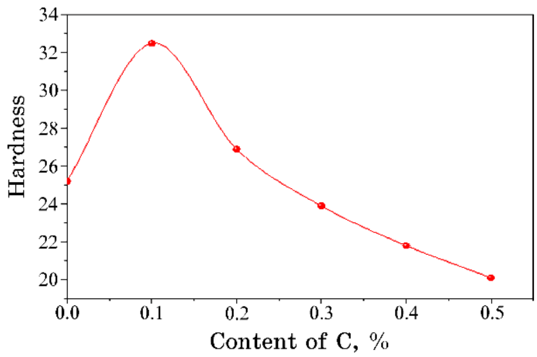

Fig. 8. Hardness curve as a function of carbon content in the samples.

value is for the second sample, as the proportion of reinforced nanocarbon constituted 0.1 g of the compressed mass. We also notice an increase in the apparent and true porosity values with the increase in the reinforcement content. The highest porosity value was for the sixth sample.

Figure 9 shows the apparent and true porosity curves as a function of the change in the reinforcement content in the compressed samples. We also notice that the true porosity is slightly higher than the apparent porosity. The clear increase in the ratio of the true and apparent porosities is attributed to the improvement of the adhesion between the base metal and the reinforcement particles.

5.3. Apparent and Bulk Density

Table 4 shows the nanocarbon content and the apparent density and bulk density values of the compressed samples. The highest density value is for the second sample. We also notice that the density values decrease with increasing the reinforcement content. The lowest density value was for the sixth sample.

Figure 10 shows the apparent density and bulk density curves as

TABLE 3. Porosity values and carbon content in the samples.

No. of samples	Content of C, %	Apparent porosity	True porosity
1	0	2.31	2.51
2	0.1	0.71	0.79
3	0.2	2.22	2.59
4	0.3	4.02	4.49
5	0.4	5.55	5.95
6	0.5	6.87	7.21

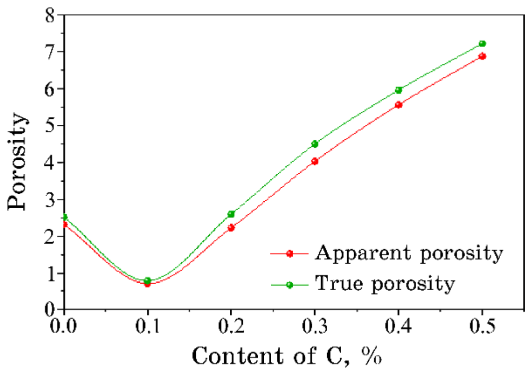

Fig. 9. Porosity curves as functions of carbon content in the samples.

functions of the change in reinforcement content in the compressed samples. We also notice that the apparent density is slightly higher than the bulk density, and the density curves change in an opposite manner to the change in the porosity curves.

6. CONCLUSIONS

This study showed that the mechanical properties of aluminium can be changed by adding nanocarbon as a reinforcement material at ratios of 0.1 g from the previous ratio to obtain six samples using the powder-metallurgy method.

It was found that the hardness increases, when sample is reinforced with a small percentage of carbon, and then begins to decrease with the increase of the reinforcement material, while the apparent porosity and true porosity increase at the lowest percentage of reinforcement and then begin to increase with the increase of the reinforcement-material content.

It was also found that the apparent density and volume density curves behave in the opposite direction to the porosity curves.

TABLE 4. Density values and carbon content in the samples.

No. of samples	Content of C, %	Apparent density	Bulk density
1	0	2.48	2.45
2	0.1	2.84	2.79
3	0.2	2.55	2.51
4	0.3	2.29	2.25
5	0.4	2.08	2.04
6	0.5	1.91	1.85

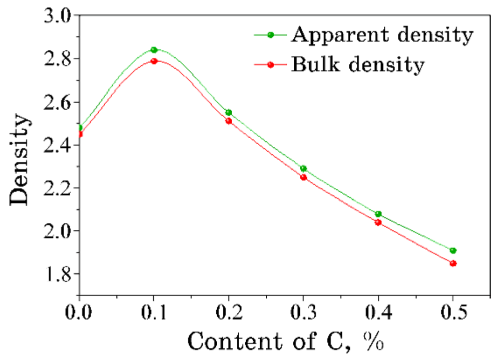

Fig. 10. Density curves as functions of carbon content in the samples.

REFERENCES

1. K. Velavan and K. Palanikumar, *Applied Mechanics and Materials*, **766**: 293 (2015); https://doi.org/10.4028/www.scientific.net/AMM.766-767.293
2. A. Jamwal, P. Prakash, D. Kumar, N. Singh, K. Sadasivuni, K. Harshit, and P. Gupta, *Journal of Composite Materials*, **53**, No. 18: 2545 (2019); https://doi.org/10.1177/0021998319832961
3. A. Saxena, N. Singh, D. Kumar, and P. Gupta, *Materials Today: Proceedings*, **4**, No. 4: 5561 (2017); https://doi.org/10.1016/j.matpr.2017.06.013
4. D. J. Woo, F. C. Heer, L. N. Brewer, J. P. Hooper, and S. Osswald, *Carbon*, **86**: 15 (2015); https://doi.org/10.1016/ j.carbon.2015.01.010
5. H. Kwon, G. G. Lee, S. G. Kim, B. W. Lee, W. C. Seo, and M. Leparoux, *Materials Science and Engineering A*, **632**: 72 (2015); https://doi.org/10.1016/j.msea.2015.02.057
6. V. I. Titov, L. V. Tarasenko, A. N. Utkina, and A. B. Shal'kevich, *Inorganic Materials*, **52**: 1461 (2016); https://doi.org/10.1134/S0020168516150164
7. Pallav Gupta, Devendra Kumar, Om Parkash, and A. K. Jha, *Bulletin of Materials Science*, **36**: 859 (2013); https://doi.org/10.1007/s12034-013-0545-1
8. J. Wang, X. Zhang, N. Zhao, and C. He, *Journal of Materials Science*, **54**, No. 7: 5498 (2019); https://doi.org/10.1007/s10853-018-03245-2
9. Mary A. Awotunde, Adewale O. Adegbenjo, Babatunde A. Obadele, Moses

Okoro, Brendon M. Shongwe, and Peter A. Olubambi, *Journal of Materials Research and Technology*, **8**, No. 2: 2432 (2019); https://doi.org/10.1016/j.jmrt.2019.01.026
10. Afsaneh Dorri Moghadam, Benjamin F. Schultz, J. B. Ferguson, Emad Omrani, Pradeep K. Rohatgi, and Nikhil Gupta, *JOM*, **66**: 872 (2014); https://doi.org/10.1007/s11837-014-0948-5
11. Karthikeyan Lakshmanan, Pitchipoo Pandian, Rajakarunakaran Sivaprakasam, and Kathiravan Sundaram, *Mechanics of Advanced Composite Structures*, **12**, No. 1: 25 (2025); https://doi.org/10.22075/macs.2024.32547.1589
12. Shakil Hossain, MD Mamunur Rahman, Devesh Chawla, Alip Kumar, Prem Prakash Seth, Pallav Gupta, Devendra Kumar, Rajeev Agrawal, and Anbesh Jamwal, *Materials Today: Proceedings*, **21**: 1458 (2020); https://doi.org/10.1016/j.matpr.2019.10.089
13. Udaya Devadiga, Sunil Kumar Shetty, and Peter Fernandes, *Materials Today: Proceedings*, **22**: 2247 (2020); https://doi.org/10.1016/j.matpr.2020.03.345
14. V. Chak, H. Chattopadhyay, and T. L. Dora, *Materials and Manufacturing Processes,* **36**, No. 11: 1219 (2021); https://doi.org/10.1080/10426914.2021.1914845
15. Bowen Xiong, Kang Liu, Wei Xiong, Xiang Wu, and Jiayi Sun, *Journal of Alloys and Compounds*, **845**: 156282 (2020); https://doi.org/10.1016/j.jallcom.2020.156282
16. M. M. Mawat, A. M. Alattar, A. N. Mohamed, and J. F. Odah, *International Scientific Congress of Pure, Applied and Technological Sciences (MINAR Congress)*, **11**: 28 (2024); http://dx.doi.org/10.47832/MinarCongress11-3
17. Sarojrani Pattnaik, *The International Journal of Advanced Manufacturing Technology*, **93**: 6919 (2017); https://doi.org/10.1007/s00170-017-0559-8
18. R. H. Al-Saqa, I. K. Jassim, and M. M. Uonis, *Ochrona przed Korozją*, **8**: 243 (2023); doi:10.15199/40.2023.8.3
19. Moustafa M. Mohammed, Elsayed M. Elsayed, Omyma A. El-Kady, Naser A. Alsaleh, Ammar H. Elsheikh, Fadl A. Essa, Mahmoud Ahmadein, and Joy Djuansjah, *Coatings*, **12**, No. 3: 409 (2022); https://doi.org/10.3390/coatings12030409